Supporting information

Shen, et. al. Architecture and inherent robustness of a bacterial cell cycle control system

Contents

There are five sections to this supporting information: (A) a summary of the molecular mechanisms that are reflected in the simulation model of the *Caulobacter* cell cycle control system, (B) a description of the simulation model, (C) an enumeration of the parameters in the model and their justification, (D) a discussion on several *in* silico mutant strain simulations, and (E) further description of the method for robustness used in this paper. Extensive data and explanations of the mutant strain simulation and mRNA concentrations predictions that validate the performance of the simulation model are available on at http://www.stanford.edu/group/caulobacter/CellModel. The source code for all models in this work is available on that site as well.

A. Summary of molecular mechanisms

In this section, we outline the molecular mechanisms that comprise the *Caulobacter crescentus* cell cycle control system. The details of the control circuitry that we analyze in the main manuscript have been characterized by many laboratories, including our own, over several decades. The goal here is to provide a roadmap to the papers where the molecular and genetic mechanisms are characterized. Table S1 lists the papers that provide the key conclusions relating to proteins in the model.

The cyclical genetic circuit comprised of the CtrA, GcrA, DnaA, and CcrM master regulatory proteins shown schematically in Fig. 1 C and D, and in more detail at the bottom of Fig. S1A, directly controls the temporal expression of over 200 genes (1-4). These proteins are present in succession as the cell cycle progresses (Fig. 1 A and B). The cascade of regulatory factors starts with DnaA accumulation at the swarmer-to-stalked cell transition. DnaA activates the transcription of multiple genes involved in DNA replication and cytokinesis as well as turning on the next gene in the cascade, *gcrA* (Fig. 1C) (3, 5). GcrA regulates genes involved in chromosome replication and segregation and turns off *dnaA* as it activates *ctrA* transcription (2). CtrA directly controls the transcription of genes required for polar organelle biogenesis and cytokinesis, while turning off the transcription of *gcrA* and activating the synthesis of the CcrM DNA methyltransferase (6). Using an elegant mechanism (7), the differential methylation state of the chromosome at different stages of the cell cycle controls expression of the components of the core cell cycle engine (Fig. 1D). This cascade of top-level master regulators creates the forward-biased, cyclical genetic circuit – the core cell cycle engine – that organizes cell cycle progression (Fig. S1). The core engine activates the subsystems that implement the cell cycle, including several complex processive reactions that take extended time intervals to complete, particularly replication of the chromosome and cytokinesis (Fig. S1). (By processive reactions, we mean reaction cascades that involve a succession of many reactions that under normal growth conditions always go to completion once the cascade is initiated.)

Processive reactions determine cell cycle timing

The forward-biased cyclical cascade comprising the core DnaA/GcrA/CtrA/CcrM cycle is tightly coupled to processive reactions (Fig. 1 C and D and S1). In the case of the stalked cell cycle (Fig. S1A), the principal processive cascades are DNA replication and the constrictive phase of cytokinesis. These two cascades are constrained by a checkpoint mechanism so that constriction only completes after chromosome replication (8). These two end-to-end reaction cascades that occur over about 100 min (black circles at the top of Fig. S1A and green boxes in Fig. 3B) are the pacing events in the stalked cell cycle. In the swarmer cell, an additional process occurs during the 20 min period of motility after cell separation as shown in Fig. S1B. The mechanisms controlling duration of the swarmer phase are currently unknown; however, since the duration of the swarmer cell phase is relatively constant across a population of synchronized cells in log growth conditions, we expect to find that another reaction cascade determines this minimum swarmer stage duration.

C. crescentus DNA replication involves two parallel reaction cascades, each with about two million reactions (the chromosome has about four million nucleotides), executed at two replication forks. The level of expression of three of the four cell cycle master regulator proteins, CcrM, CtrA and DnaA, is coupled to the progression of DNA replication by the DNA methylation-state change that occurs upon passage of a replication fork over their respective genes (7, 9, 10). The *dnaA* gene is transcribed preferentially from a fully methylated promoter. This methylation state control of *dnaA* transcription is of particular interest owing to DnaA's central role in the initiation of chromosome replication. The *dnaA* gene is near the chromosomal origin of replication (*Cori*), and upon passage of the replication fork it becomes hemimethylated, and thus down-regulated (7). The enzyme that remethylates DNA, CcrM, only accumulates near the completion of DNA replication, and it is then rapidly both deactivated and cleared from the cell (11, 12). Remethylation of the chromosome by CcrM near the end of replication enables *dnaA* transcription in preparation for the next cell cycle. (In many bacteria, including *E. coli*, the DNA methylase is not cell cycle dependent.) This and other mechanisms controlling DnaA and CtrA activity assure that there is one and only one round of replication per cell cycle.

Asymmetric cell division depends on polar localized regulatory proteins and cytoplasmic compartmentalization

The constriction of the FtsZ-ring that divides the cell is a complex cascade involving a changing set of many proteins (13). Constriction is dependent on presence of the CtrA~P-activated FtsA and FtsQ proteins (14, 15). Constriction is first apparent late in chromosome replication and cell separation occurs about 25 min after completion of replication. In *C. crescentus* cells, there are two constrictive mechanisms late in cytokinesis, one for the inner, and one for the outer, cell membrane. The inner membrane fissions about 20 min before completion of outer membrane constriction to divide the cytoplasm into two compartments (16, 17). This cytoplasm compartmentalization event triggers elimination of CtrA~P in the nascent stalked cell compartment, which both enables activation of DNA replication and precipitates major changes to the transcriptome since CtrA~P directly regulates transcription of about 95 genes (1, 18-20). Dynamic localization of regulatory proteins and proteolytic subsystems to the cell poles is essential to asymmetric cell division (4, 21). Immediately upon compartmentalization, differentiation begins owing to isolation of key phosphorylation dependent regulatory proteins

from their cognate kinases (19, 22, 23) and/or perhaps to differential sequestering of a phosphatase (20). Large differences in binding affinity between the phosphorylated and unphosphorylated response regulators in the nascent daughter cell compartments cause gene expression profiles to diverge, and thus, differential development programs can proceed thenceforth, with profound consequences for the fates of the two daughter cells. Cytoplasmic compartmentalization disrupts the distributed phosphosignaling network involving localized CckA histidine kinase and cytoplasmic ChpT phosphotransferase to trigger rapid elimination of activated CtrA~P from the nascent stalked daughter cell so that chromosome replication can initiate (19, 20, 24). In contrast, elimination of CtrA~P from the swarmer cell is delayed until about 20 min after daughter cell separation when the CckA/ChpT pathway is disrupted by another mechanism. The distinctive identity of the subsequent daughter cells, each containing one of the chromosomes of the predivisional cell, begins at the instant of cytoplasmic compartmentalization (17).

B. Simulation Model Description

This section describes the simulation model of the *C. crescentus* cell cycle control system (Fig. S2) and the equations used to model the operation of each component of the control system.

Fig. S2A provides a graphic picture of events that occur in the course of a *C. crescentus* cell cycle starting from a newly separated swarmer daughter cell on the left. The events are scaled to a nominal 135 min cell cycle. (In practice, even in a population with average doubling time of 135 min, there will be a wide distribution of generation times for the cells within the population.) The normal environment of *C. crescentus* is clear lakes and streams where nutrients are dilute and long periods of extremely low levels of nutrients or even starvation are common. As described in the main text, the cell cycle control system of *C. crescentus* is designed to function well over a wide range of generation times, including mechanisms to halt cell cycle progression in times of carbon or nitrogen starvation and to restart gracefully when these nutrients are again present.

Model architecture

Here we only included details of timing and control of chromosome replication and cytokinesis because progress of these two subsystems is essential to progress of the cell cycle engine. The simulation model has a hierarchical architecture that mimics the organization of the cells regulatory control system (Fig. S3). The simulation is constructed using the Matlab Simulink (25) and Stateflow (26) tools that are widely used by control engineers to design, analyze, and simulate control systems. Simulink is a Matlab-integrated platform for simulation and design of dynamic systems with an interactive graphical environment. Stateflow is tightly integrated with Matlab and Simulink, and it is used to model event-triggered changes in simulation parameters during progression of the simulation. The combination of Simulink and Stateflow gives an interactive simulation tool well suited for modeling of hybrid dynamic systems, that is, systems that include some elements describable by ordinary differential equations (ODEs) and other elements that are more switch like. This combination of features is well matched to requirements for simulation of the *C. crescentus* cell cycle control system. In addition, the modular architecture of models constructed with Simulink and Stateflow will facilitate extension of the *C. crescentus* cell cycle model to add additional mechanistic details as they are reported and to

extend the cell cycle model to incorporate environmental sensor/response systems that affect operation of the cell cycle. Thus, this extensible modeling paradigm provides an approach applicable to construction of a whole cell model. The simulation files are available at http://www.stanford.edu/group/caulobacter/CellModel.

The top level Matlab model file (Caulobacter.mdl) includes two major blocks: The Simulink subsystem models the core oscillatory circuit comprised of DnaA, GcrA, CtrA, and CcrM regulatory proteins and a parsimonious additional set of proteins (DnaB, FtsZ, and FtsQA) that are in the pathway for control of two key controlled subsystems, DNA replication and cell constriction. The Stateflow subsystem monitors progress of the Simulink cell cycle simulation to detect conditional events, and it contains phenomenological models of the operation of the two controlled processive subsystems. For example, the conditions to initiate DNA replication in the model are (DnaA AND DnaB) NOT CtrA (see the green box in Fig. S2B). (This logic is an abstraction representing necessary, but not necessarily sufficient, conditions for initiation of replication.) The Stateflow subsystem monitors the changing levels of the various proteins modeled by the Simulink subsystem and detects satisfaction of the "initiate replication" conditions. When the "initiate replication" event is detected, the Stateflow model of DNA replication progression is initiated. Key outputs from this model are the timing (in the simulation) of replication of *dnaA*, *ctrA*, and *ccrM* genes. At the time of their replication, the promoter regions of these genes become hemimethylated. Their hemimethylation status is signaled to the Simulink model where it affects the rate of expression of the these genes (7).

The Simulink system is an ordinary differential equation (ODE) solver with a graphical interface. Rates of protein synthesis and proteolysis and phosphorylation reactions within the regulatory protein circuit of the cell cycle engine are all modeled in Simulink as a system of ODEs. Principal outputs of the Simulink subsystem are estimated protein and mRNA levels versus time in the cell cycle. These changing protein levels and the cell cycle time are inputs into the Stateflow subsystem. The outputs of the Stateflow subsystem are values for binary switched parameters in the simulation model in the Simulink subsystem. Stateflow provides the capability to change parameter values in the ODEs in Simulink as the simulation progresses, that is, as the equations are being numerically integrated. As described above for the promoter methylation states and conditions for initiation of DNA replication, the Stateflow subsystem monitors the current (in simulation time) values of protein levels and switches the parameters when some condition is satisfied. Stateflow can also switch parameters at designated time points (in simulation time) during simulation. Examples of switched parameter values provided to Simulink by the Stateflow subsystem include the DNA methylation state of methylation-dependent promoters and the cell stage (swarmer, stalked, or predivisional) that is used in Simulink to sets protein half-lives to the values experimentally observed in synchronized cell populations.

General modeling considerations

We are modeling events and chemical reactions as they occur in a single cell reaction chamber. The phenomena leading to stochastic reaction rates and variations in progress of cell cycle events are not considered in this cell level simulation. However, the effect of stochastic variations in rates of progression of chemical cascades on the *C. crescentus* cell cycle is to cause dispersion in timing of events over the cell population, which we can reflect by convolving the single cell

predictions of the protein and mRNA concentrations profiles with a Gaussian function. The results of the convolution approximate the corresponding experimentally observed dispersion patterns from cell population measurements. These convolved protein and mRNA profiles can then be compared to experimental results from Western blots or micro-array mRNA assays on cell populations as in Fig. 2.

Models in the Simulink subsystem

Where we know genetic mechanisms and bio-chemical reactions, we use explicit or approximate kinetic models in the form of ODEs in the Simulink subsystem. Where we do not know details, but we do know phenomenology such as signal timing or the average time to complete a process, phenomenological models were constructed within the Stateflow subsystem. An example is the model of the CckA-originated phosphosignal that controls CtrA proteolysis and its phosphorylation state. From experimental observations, we know that this signal is interrupted at the time of cytoplasmic compartmentalization (17, 27) and at the swarmer-to-stalked cell transition. We also know the timing of these two events and the timing of reactivation of the phosphosignal path in the predivisional cell from experimental observation. We define a conditional event in Stateflow to switch this CckA-originated phosphosignal off and on in the Simulink simulation at the appropriate times. (The robustness analysis described in the main text investigated sensitivity to specific timing of the CckA phosphosignal and found that the architecture of the cell cycle control circuit provides for successful completion of the cell cycle even when the specific timing of this signal varies over a wide range.) This phenomenological modeling approach enables realistic simulation of the known circuitry and phenomenology even though biochemical mechanisms in the pathway are still incompletely characterized.

Table S2 shows the models within the simulation governing regulation of protein synthesis, proteolysis and activation. Stochastic effects are neglected in the single cell model as noted above. The level of promoter activation (as a fraction of the maximum activation) is modeled using functions based on a Hill function approach. Protein production (nM/second) is modeled by a multiplicative constant representing the maximum synthesis rate, times the fractional promoter activation. This is equivalent to assuming a constant average rate of protein production per mRNA. The effects of promoter methylation states are included in the promoter activation models, as are the cases where there are multiple promoters or multiple regulatory ligands. Instantaneous values for the binary switch parameters in the ODEs (e.g., the methylation state of a promoter) are determined by the Stateflow subsystem. Proteolysis is modeled by an exponential decay function with a half-life parameter. The timing of initiation of CtrA proteolysis is determined by the Stateflow controlled phosphosignaling pathway originating at CckA. In other cases where there is experimental data for different half-lives at different cell cycle stages, the respective half-life parameters are set to the observed values (by input from the Stateflow subsystem) as the cell cycle progresses.

The model predicts the changing intracellular concentration of the regulatory proteins and mRNAs. We assume that the effects of growth in the cell volume can be neglected. Cell growth causes continuous dilution of the protein concentration and is thus computationally similar to a protein degradation term with half-life equivalent to the cell generation time (assumed to be 135 min). Since regulatory protein half-lives are observed to be much less than the generation time, this dilution effect is negligible. In the case of protein synthesis, a gene producing a constant

average rate of molecules/second would produce twice the incremental protein concentration/sec (nM/sec) in the small initial cell compared to the rate per gene in the larger cell near cell division. However, over the course of the cell cycle, each gene is duplicated so that the gene dosage is doubled and thus the rate of protein production from activated genes is also doubled compensating for the larger cell volume.

In the model equations in Table S2, protein and mRNA rates are in nM/sec. Where necessary conversions between molecules/sec per cell and nM/sec per cell were made using

$$\text{M molecules/sec} = \frac{M}{A_g \cdot V_{avg}} \text{nM/sec}$$

where A_g is Avagodro's number in nmol^{-1} and V_{avg} is the average value over the cell cycle of the *Caulobacter* cell volume in liters. Using 7.5×10^{-16} liters (0.75 μm³) for V_{avg}, the conversion factor $\frac{1}{A_g \cdot V_{avg}}$ is 2.2. Since we simulate the molecular concentrations instead of the number of molecules/cell at the time of compartmentalization, concentrations of cytoplasmic proteins are initially equivalent in each of the new compartments. Polar localized proteins can have significantly different concentrations in each compartment, however, which can differentially affect the subsequent evolution of the respective biochemical and genetic systems of the compartments.

We compare our simulation prediction to experimental values obtained from Western blots. Each time point of the Western blots was normalized to the same cell mass (OD660nm) to facilitate comparisons with the *in silico* simulation predictions.

Additional assumptions:

1. No phosphatase signal. There could be a phosphatase signal that works in conjunction with the CckA phosphosignal to accelerate dephosphorylation of CtrA (19, 20). If such a mechanism exists, it would increase the speed and reliability of elimination of CtrA~P.

2. After the initiation of chromosome replication, there is a time window when DnaA is still present but CtrA is not yet re-synthesized. During this interval, we assume that there exists a mechanism to prevent excessive chromosome replication initiation in *C. crescentus.* The mechanism might involve control of the level of activation of DnaA by ATP as with *E. coli* DnaA.

Models in the Stateflow subsystem

The Stateflow subsystem includes models of four physical processes: cell stage, the CckA phosphosignal state (i.e., ON or OFF), the progression of chromosome replication, and the progression of cytokinesis (Fig. S4). Chromosome replication and cytokinesis are processive models, that is, complex biochemical reactions that take extended time intervals to complete. The chromosome replication model computes the fractional completion of replication as a function of time after initiation, assuming a linear rate of replication. This model also determines the DNA methylation state of the promoters whose activity is affected by methylation and provides a

corresponding input signal to the genetic circuit model and the Simulink subsystem. The fractional completion of cytokinesis is also modeled with a linear model that signals when cytoplasmic compartmentalization occurs and when daughter cell separation occurs.

Over a cell cycle, Stateflow functions as follows[*]:

1. The cell is initially in the swarmer cell state (set *isSW* to 1).

2. At 20 minute in simulation time (minSim), the cell transitions from the swarmer stage into the stalked stage (set *isSW* to 0 and set *isST* to 1).

3. During the transition, the CckA phosphosignal is switched to start CtrA proteolysis by the ClpXP machinery (set *clpXP* to 1).

4. When the CtrA level becomes low (through proteolysis) while the DnaA and DnaB levels are still high, chromosome replication is initiated.

5. Chromosome replication is modeled as a linear process lasting 80 minutes. When a fully-methylated promoter is replicated, it becomes hemi-methylated. Starting from the *ori*, the simulated progression of the replication fork reaches the *dnaA, ctrA,* and *ccrM* genes (at a time depending upon their position on the chromosome) and successively switches *mdnaA*, *mccrM,* and *mctrA* from 0 to 1 to indicate the promoter is then hemimethylated. Hemi-methylation reduces *dnaA* expression while, it enables *ctrA* and *ccrM* expression.

6. At 80 minSim (60 minSim into chromosome replication), the phosphosignal activates CckA again, switching *cckA* to 1.

7. The Simulink model starts to synthesize CtrA again when *mctrA* is set to 0. When *cckA* is switched to 1, CtrA is phosphorylated into CtrA~P, the active form of CtrA, which activates the *ftsQA* promoter to synthesize FtsQ and FtsA.

8. FtsQ and FtsA are required to start cytokinesis (14). Cytokinesis is modeled as a linear process that lasts 30 minutes from start of cell constriction to cell separation, with cytoplasmic compartmentalization occurring 18 min (17) before cell separation.

9. The cell cycle stage is changed from stalked to pre-division when cytokinesis starts (set *isPD* to 1 and *isST* to 0).

10. 80 minSim after the replication is initiated, chromosome replication completes and the two chromosomes are separated. *chro_rep* is reset to 0 again.

11. 12 minSim into cytokinesis, the inner membrane of the cell fissions, and the cytoplasm is compartmentalized. Chromosome replication has to complete before compartmentalization can take place, so the simulation checks if *chro_rep* has been reset to 0 before allowing compartmentalization to happen.

12. Upon compartmentalization, the CckA phosphosignal is blocked in the nascent stalked daughter cell (set *cckA* to 0). The disappearance of the CckA phosphosignal activates CtrA proteolysis by the ClpXP machinery (19) (set *clpXP* to 1).

---

[*]   Specific numbers shown are parameterized in the simulation and could vary depending upon the particular case being studied.

13. 30 minSim after the initiation of cytokinesis, the two daughter cells are separated.

C. Parameters

The cell cycle simulation model has a total of 62 parameters. Among them, 29 parameters have experimentally measured values (Table S3A), 25 parameters have estimated nominal values (Table S3B), and 9 parameters are used for *in-silico* mutant simulations (Table S3C). The robustness analysis as described in the main text found that the cell cycle control circuit design will execute the cell cycle correctly over wide ranges of parameter values.

We use data from (28) scaled to a 135 min swarmer cell generation time for the timing of the swarmer cell stage, and chromosome replication. With the exception of CtrA and CcrM, *in vivo* measurements of the number of protein molecules in the *C. crescentus* cell have not been published, and *in vitro* studies to measure ligand-promoter binding kinetics are only available for a few CtrA binding sites (29, 30). Accordingly, we normalize protein concentrations (from quantified Western blots) to the maximum concentration, and we assume that all promoters are activated at a small fraction of the peak level of the activating ligand(s). We used a parameterized Hill-function type model of gene activation that yields good agreement between observed (normalized) mRNA temporal profiles from microarray assays and predicted values from the simulation (http://www.stanford.edu/group/caulobacter/CellModel, Table S2). Half-lives of DnaA, GcrA, and CtrA have been experimentally determined in swarmer cells and stalked cells(5, 27, 31), and the active regulation of CtrA proteolysis as a function of the cell cycle has been extensively studied(18, 19). The relatively small dilution effects of cell growth are assumed to be included in the experimental protein half-life data. Pathways controlling DnaA and GcrA stability have not been characterized, so we modeled the observed dynamic control of DnaA and GcrA stability by setting their half-lives to the reported value at each stage in the cell cycle. Time-resolved measurements of protein phosphorylation states are possible, but with poor resolution, and *in vivo* kinetics of *C. crescentus* phosphorylation reactions are not available. We assume that the phosphosignaling reactions are fast enough that phosphorylation-related switching is much faster than switching by genetic mechanisms or protein degradation. The rationale for choice of all parameter values is in Section C.

Naming conventions for Hill function parameters are as follows:

The default value of Hill coefficient *n* for all promoters is denoted by hcDef (In the current model, all the promoters share the same default Hill coefficient value). The default concentration of a transcriptional factor ($[C_d]$) that yields half-maximal expression is denoted by cHalfDef. The concentration of CtrA~P that yields half-maximal expression in the CtrA~P-regulated genes is different from the default value cHalfDef and is denoted by cHalfCtrA. The maximum protein synthesis rate divided by the cell volume, *β/V,* is converted to nanomolar per second (nM/s) and denoted by pX for protein X. The half-life of protein X is denoted by hlX. The initial concentration of protein X is denoted by cX0.

For comparison to experimental values, estimated protein concentration profiles are normalized to a peak value of one, and experimental values are normalized the same way. Ligand activation levels at downstream binding sites are assumed to be a small fraction of the peak concentration of that ligand.

Concentration vs. number of protein molecules per cell

In the model, we chose to simulate the concentration levels rather than the number of protein molecules per cell. The number of protein molecules per cell is converted to the protein concentration, using:

$$[C] = \frac{M}{A_g \cdot V_{avg}} \qquad (1)$$

Where $[C]$ is the protein concentration in nM (nmol/L), M is protein molecules per cell, A_g is the Avogadro's number (6.022×10^{14} nmol^{-1}), and $Vavg$ is the average volume over a cell cycle of a *C. crescentus* cell in liters.

During cell cycle progression, the *C. crescentus* cell grows larger. In the simulation, we used the average volume of the *C. crescentus* cell to calculate the molecular concentrations. The doubling of the cell volume over the cell cycle is compensated by the doubling of gene copy number as well by DNA replication. The dilution of protein concentration by growth is comparable to a 135 min half life (for our assumed swarmer cell cycle time) which is well longer than the regulatory protein half lives and thus can be neglected.

During cell cycle progression, the volume of a *C. crescentus* cell grows from around 0.5 μm^3 in early swarmer stage to around 1.2 μm^3 in pre-divisional stage. We take 0.75 μm^3 as V$_{avg}$.

Therefore, $[C] = \dfrac{M}{A_g \cdot V_{avg}} = \dfrac{M}{6.022 \times 10^{14} \cdot 7.5 \times 10^{-16}} = 2.2M$ (nM) $\quad$ (2)

Notes for Table S3B -- parameters with estimated values

Measurements of these parameters are currently unavailable so we estimated nominal values. The simulation predictions are not sensitive to most of these parameters for reasons outlined below.

These parameters fall into six categories.

1. Initial regulatory protein concentrations

    The cell cycle simulation is relatively insensitive to these initial levels, because after one or two simulated cell cycles the concentrations in swarmer cells stabilize with other values which are determined by other parameters in the model.

2. Protein concentration ranges of action (or thresholds) that control cell functions such as DNA replication, cytokinesis and DNA methylation.

    Many cell functions are initiated when a regulatory protein is synthesized and its level rises about a range of action at a downstream binding site. We selected the thresholds to be well

below the peak levels (assumed to be the usual situation for bacterial genetic regulatory links). Change in an assumed threshold value will change the time of a regulatory reaction. The sensitivity of cell cycle outcome to timing variations was explored and shown to be low as part of the robustness analysis as described in the main text.

3. Protein synthesis rates from an activated gene

The protein synthesis rate depends on both the rate of transcript initiation and the average number of proteins produced from each mRNA. Both these rates vary in both average values for different genes and stochastically between cells in a population at any given instant. We used nominal synthesis rates chosen to be representative for bacterial promoters. Differences in actual values would affect delays in downstream gene activation or repression and the peak values of protein concentrations in the simulation. Since comparisons to experimental values are done by comparing the pattern of normalized predicted and experimental values, the peak concentration values are not significant. Doubling of gene dosage and offsetting dilution by cell growth are also factors to be considered. Our confidence in this approach was reinforced by the agreement between the simulation predictions of patterns of mRNA and protein concentrations with experimental values (Fig. 2 and http://www.stanford.edu/group/caulobacter/CellModel). Further, the robustness analysis showed that the cell cycle circuit design has evolved by selection to be insensitive to variations in signal pathway timing.

4. Hill function parameters

We used the same concentration for half-maximal expression for all proteins except for CtrA as a transcriptional factor, for which we used a slightly higher concentration for half-maximal expression, based on the measured concentration of CtrA in the *C. crescentus* cell.

We used a Hill coefficient equal to 2 for all protein regulators.

5. Protein half-lives

The half-life of DnaB has not been experimentally measured. Furthermore, DnaB represents a collection of replication initiation proteins. As long as this half-life value is not extremely small, it has no effect on the simulation outcome. In other words, as long as DnaB or the other replication initiation proteins it represents are not degraded too rapidly during the initiation of chromosome replication (~ 5 minutes), the model is not sensitive to this value.

6. Rate constants for phosphorylation of CtrA

Phosphorylation is assumed to be fast relative to protein synthesis and degradation and thus to act as a rapid switch, so within this constraint the simulation is not sensitive to the specific phosphorylation rate parameters.

D. *In silico* mutant strain simulations

This section describes *in silico* mutant strain simulations that emulate several laboratory *C. crescentus* mutant strains. The objectives of these comparisons were to validate the simulation

model and to understand the reasons for the experimentally observed phenotypes in greater depth. Additional details of these simulations including graphs of the *in silico* simulation datasets are online at http://www.stanford.edu/group/caulobacter/CellModel.

Table S4 shows the four mutants that were simulated and the changes that were made to the wild-type model to create the mutant simulation. In each case, the simulation predicts (i) the concentration profile of each protein in the model in single cells as a function of cell cycle time when followed into either the swarmer or the stalked compartment of the predivisional cell, (ii) whether the cell can progress through each stage of the cell cycle, and (iii) whether DNA replication and cytokinesis occur normally.

The simulation predictions for all cases checked were consistent with the *in vivo* phenotypes. Simulation results and their relation to the mutant strains in Table S4 are as follows: *GcrA depletion strain*: The simulation predicts that CtrA~P will not re-accumulate after the stalked cell stage, so FtsQA does not accumulate enough to initiate cytokinesis. As a result, the cell cycle arrests at the stalked cell stage in the simulation. The simulated levels of DnaA and CtrA suggest that DNA replication may still happen in these cells before cell death. *Strain with constitutive accumulation of CcrM*: The simulation predicts that the re-accumulation of CtrA in pre-divisional cells will be delayed ~20 minutes, while DnaA will accumulate at high concentrations throughout the cell cycle. This suggests that over-initiation of DNA replication may take place in these mutant cells as is observed experimentally. As a consequence, the re-accumulation of FtsQA and cytokinesis will be delayed. Strain with c*onstitutive accumulation of CtrA~P*: The simulation predicts that accumulating CtrA~P will block the initiation of DNA replication. Since cytokinesis is blocked when DNA replication is blocked, the cells will arrest after the stalked cell stage as observed *in vivo*. *Strain with the ctrA gene moved next to the DNA replication terminus*: The simulation predicts that CtrA re-accumulation in predivisional cells will be delayed by ~15 minutes as is observed. As a consequence, the synthesis of FtsQA and cytokinesis will also be delayed, so that the cell cycle will be slightly longer than for wild-type cells. The consistency between the predictions from simulation of the *in silico* mutants and the *in vivo* phenotypes (Table S4) provides additional evidence that our model corresponds to the biological cell cycle control circuitry. Moreover, the predictions from *in silico* mutant simulations provide quantitative insights into how the cell cycle is affected by a given mutation.

The simulations are performed using the Matlab-based simulation of the wild-type *C. crescentus* cell cycle control system. We use the same differential equations, parameter values, and initial conditions as for wild-type cells, except for those parameters that are changed to simulate a mutation of interest. Time varying intracellular concentration levels are predicted for the eight different proteins included in the model.

1. GcrA depletion strain

C. crescentus mutant previously constructed

A mutant strain expressing the *gcrA* gene conditionally was previously constructed (2). In this strain (Δ*gcrA* P*xyl*::*gcrA*), the *gcrA* gene was deleted from its native location on the chromosome, but the strain carries a copy of the *gcrA* gene under the control of the xylose-inducible P*xyl* promoter. When a this mutant strain is grown in a media containing glucose,

which turns off the P*xyl* promoter, all cells in the population are arrest as stalked cells, and finally die about 6 hours after the switch to glucose media. It was also observed that CtrA levels become very limiting before cell death, while DnaA levels increase, when GcrA is depleted.

Changes of model parameters to simulate this mutant

To simulate this mutant *in silico*, we used the same equations (Table S2), the same initial protein concentrations, and the same parameters (Table S3A and S3B) as for wild-type cells, except that we changed the value of the "pgcrA" parameter (maximum GcrA synthesis rate from the *gcrA* promoter) in Table S3C from 6.9 nM/s to 0 nM/s at time 0 min.

Results of the mutant simulation

In this mutant simulation, we observed that the levels of GcrA remain null at all times of the cell cycle, which prevents the activation of the *ctrA*P1 promoter by GcrA in stalked cells, and therefore the re-accumulation of CtrA after the stalked cell stage of the cell cycle. As a consequence, CtrA is not present in cells after the stalked cell stage so it cannot activate the synthesis of CcrM and FtsQA. The absence of FtsQA after the stalked cell stage blocks progression of cell constriction, so the cells cannot become pre-divisional cells. All these results are in agreement with the phenotype observed *in vivo* (2) and the simulation helps explain, at a molecular level, how the cell cycle of a single cell is arrested at the stalked cell stage *in vivo* when GcrA is depleted.

We also observed that the minimal levels of DnaA and DnaB during the mutant cell cycle are not as low as the wild-type cells, while the CtrA~P level is insignificant after 40 minutes into the simulation. Since the levels of DnaA and DnaB are over the minimal values required for DNA replication ("cChroDnaA" and "cChroDnaB" are above 1380nM), we predict that it could lead to over-initiation of DNA replication events in the arrested stalked cells. The model does not simulate such events, because of the assumption that no event of initiation of DNA replication could take place if CtrA cannot re-accumulate in cells after the stalked cell stage.

2. *ccrM* constitutively expressed

C. crescentus mutant previously constructed

A mutant strain that expresses *ccrM* constitutively was previously constructed (32). This strain contains a second copy of the *ccrM* gene under the control of the constitutive P*lacZ* promoter integrated at the *ccrM* locus on the chromosome. These mutant cells are sometimes longer than wild-type cells, they sometimes constrict asymmetrically, and their cell cycle is slightly slowed down. These cells also often accumulate more than two chromosomes, showing a defect in the control of chromosome replication initiation.

Changes of model parameters to simulate this mutant

To simulate this mutant *in silico*, we used the same equations (Table S2), the same initial protein concentrations and the same parameters (Table S3A and S3B) as for wild-type cells, except that we added a constitutively activated promoter by setting the "pccrMoe" parameter (CcrM

synthesis rate from the constitutive promoter) in Table S3C to a value greater than 0. In the simulation shown here, "pccrMoe" was set to 100nM/s at time 0 min.

Simulation result: Tracking the stalked compartment:

In this mutant simulation, we observed that the levels of the DNA methylase CcrM remain high at all times of the cell cycle, which maintains the *dnaA* and the *ctrA*P1 promoters fully-methylated at all times during the simulation. As a consequence, the re-accumulation of CtrA in pre-divisional cells is delayed ~20 minutes, while the DnaA accumulates at high concentrations throughout the cell cycle.

The delayed re-accumulation of CtrA~P in pre-divisional cells in turn delays the accumulation of FtsQA, which delays progression of cell constriction during the mutant cell cycle, compared to the wild-type cell cycle. Since progression of cell constriction is delayed, the overall mutant cell cycle is ~20 minutes longer than the wild-type cell cycle in our simulations, which is in agreement with the phenotypes observed *in vivo* (32). Although the simulation model does not simulate cell growth, we predict that mutant cells will be elongated since their cell cycle is slower but their growth should not be affected compared to wild-type cells. This logical prediction is also in agreement with the phenotypes observed *in vivo*.

The high accumulation of DnaA in the mutant simulation promotes the accumulation of DnaB at a concentration which is above the minimal threshold that is necessary for the initiation of DNA replication ("cChroDnaB" is 1380 nM). The high accumulation of DnaA and DnaB, together with the delayed accumulation of CtrA~P, could promote additional initiation of DNA replication events in these mutant cells. This quantitative simulation would explain why multiple chromosomes are observed to accumulate in mutant cells *in vivo* (32).

Simulation result: Tracking the swarmer compartment:

In this mutant simulation, we observe that the levels of CcrM remain high at all times of the cell cycle, except in swarmer cells. Since DNA replication is still efficiently repressed by CtrA~P in swarmer cells ("cChroCtrA" is 345nM), the chromosome is never hemi-methylated by the passage of the replication fork in swarmer cells, even if the CcrM DNA methylase does not accumulate efficiently in swarmer cells. Like during the stalked compartment simulation, the *dnaA* and the *ctrA*P1 promoters are maintained fully-methylated at all times of the cell cycle, so the results of the phenotype simulations are comparable when following both compartments of the cell.

3. Permanently phosphorylated and stable CtrA

C. crescentus mutant previously constructed

A mutant strain producing a constitutively active and stable mutant CtrA protein was previously constructed (27). This strain contains a high copy-number plasmid carrying a mutant *ctrA* gene that encodes a *ctrAD51EΔ3Ω* (pXylX::ctrAD51EΔ3Ω) mutant protein. CtrAD51EΔ3Ω is active at all time without phosphorylation, mimicking CtrA~P, and is not subject to proteolysis by ClpXP. These mutant cells showed a dramatic increase in the population size of G1 cells and a corresponding decrease in the population size of G2 cells, indicating that DNA replication

initiation is blocked in most cells. Prior to cell death, cells continued to elongate, forming filaments.

Changes of model parameters to simulate this mutant

To simulate this mutant *in silico*, we used the same equations (Table S2), the same initial concentrations and the same parameters (Table S3A an S3B) as for the wild-type cells, except that "isAlwaysCtrAP" (a binary switch) in Table S3C was set to 1 and "hlCtrAf" (the half-life of CtrA during active proteolysis by ClpXP) was set to a value greater than "hlCtrAc" (the half-life of CtrA without active proteolysis), 200 min in this case.

Results of the mutant simulation

In this mutant simulation, we observed that the levels of CtrA~P increase very fast after the two switches were changed, and then remain high at all times of the cell cycle. Since the levels of CtrA~P are above the maximum threshold to allow the initiation of DNA replication ("cCroCtrA" is 345 nM), the replication of the chromosome is not initiated during the swarmer-to stalked cell transition, even though the levels of DnaA and DnaB are higher than in wild-type cells. We also observed that the levels of FtsZ and FtsQA are higher in the mutant cells than in wild-type cells, but progression of cell constriction is not initiated in the G1 arrested cells, because we have made the assumption that progression of cell constriction is blocked until the replication of the chromosome is complete in our model. Still growing but not able to divide, we predict that the cells will become elongated and filamentous before they die. Hence, this *in silico* mutant simulation agrees with the *in vivo* phenotypes and helps explain what is happening in the cell at a molecular level.

4. Move the *ctrA* gene to a chromosomal position next to the terminus

C. crescentus mutant previously constructed

The *ctrA* gene is located at a chromosomal location next to the origin of replication, and its transcription is activated when the *ctrA*P1 promoter becomes hemi-methylated by the passage of the replication fork, soon after the initiation of replication. A mutant strain was constructed (10), where the *ctrA* gene was moved to a position next to the terminus, and deleted at its native position. The distribution of length of these mutant cells was somewhat broader than the distribution of wild-type cells, and the re-accumulation of CtrA in early pre-divisional cells is delayed for ~15 minutes.

Changes of model parameters to simulate this mutant

To simulate this mutant *in silico*, we used the same equations (Table S2), the same initial protein concentrations and the same parameters (Table S3A an S3B) as for the wild-type cells, except that we changed the value of the "zpctrA" parameter (the relative location of the *ctrA* gene on the chromosome) in Table S3C from 0.3 to 1.

Simulation results: Tracking the stalked compartment:

In this mutant simulation, we observed that CtrA~P re-accumulation in pre-divisional cells is delayed by ~15 minutes, because the *ctrA*P1 promoter is kept fully-methylated for a longer time period of the cell cycle. This result shows that our model is very quantitative, since it simulates the same delay in CtrA re-accumulation as observed *in vivo* (10). We also observe that the delay in CtrA re-accumulation retards the accumulation of FtsQA, which delays progression of cell constriction by ~15 minutes. Overall, the cell cycle of stalked cells now takes ~125 minutes to complete instead of ~115 minutes for the wild-type stalked cell cycle.

Simulation results: Tracking the swarmer compartment:

We observed that the results of the phenotype simulations are comparable when following both compartments of the cell. Overall, the cell cycle of swarmer cells now takes ~150 minutes to complete instead of ~135 minutes for the wild-type swarmer cell cycle.

E. Analysis of robustness

This section describes the robustness analysis of the *C. crescentus* cell cycle control circuitry using symbolic model checking, a method we adapted from electrical circuit design. First, the concept of timing analysis of the *C. crescentus* cell cycle as a finite state system is described. Then we describe how the cell cycle model was converted into a format readable by NuSMV (33, 34), a tool for symbolic model checking. Timing analysis has long been used in engineering to check the robustness of electrical circuits, and to determine if the circuit will always generate the correct logic outcome regardless of its environment and random variation in parameter values. NuSMV was used to check the robustness of the *C. crescentus* cell cycle control circuit to identify hazardous conditions, that is, potential situations where the circuit might not complete the cell cycle.

At any particular time point during the cell cycle, multiple reaction pathways are active in parallel, and depending on the relative speed of the reactions, the cell cycle could potentially end up in different states. In the discrete logic description of the regulatory network (see the main text), the discrete expression level of each promoter is controlled by the discrete levels of its transcriptional factors. The expression level determines the discrete level of the protein being synthesized, but with an arbitrary delay. Other non-transcriptional reaction characteristics such as phosphorylation state and proteolysis are also treated as discrete variables. The states of other cell cycle processes such as DNA replication and cell constriction from the simulation model are also described by sets of discrete variables. The discrete logic version of the cell cycle control circuit defines the logical relationships, and the symbolic model checking tool explores the effect of timing variations, by evaluating all possible ordering of transitions. By trying all options, the tool iterates over all possible ordering of the transition events, thus ensuring that all possible timing variation effects are investigated. As described in the main text, the exploration of event timing space is equivalent to exploring the space of biological parameters that determine the timing. As it explores these transition orders, it also checks that the user defined constraints defining correct execution of the cell cycle are met (see below). The tool reports to the user any transition order that violates these constraints.

NuSMV timing analysis

In the NuSMV input language, a system is described as a collection of state variables ranging over finite sets of discrete values representing states, along with rules for updating these variables as the system progresses through different states. A state variable is assigned to represent the state of chromosome replication, which can take on different discrete values indicating pre-replication, initiation of replication, and the middle of replication. A progression of states of the system through time is called a path and the system may be able to progress through many possible paths. In NuSMV, a state may have many alternative successor states. To search for timing hazards in the cell cycle control circuit, the NuSMV state-updating rules were written to choose nondeterministically between changing states and waiting, resulting in scenarios for every variation in reaction speeds possible within the model. Some signaling pathways (e.g., phosphosignaling) are assumed to be much faster than signaling by synthesis and degradation of protein concentrations. To distinguish between processes operating at different time scales, we used slow state update rules with arbitrary delays for the protein-level signaling, and immediate rules for phosphosignaling pathways.

NuSMV uses symbolic analysis of the branching graph of all possible paths to check whether all of the possible behaviors of the system satisfy a specified behavioral property written as a temporal logic formula called CTL (for "Computation Tree Logic"). For example, one can specify that the cell cycle has to pass through a particular set of states in a specific order to complete a cell cycle. All paths corresponding to successful completion of the cell cycle have to satisfy the CTL formula defined by the user for the system under examination. NuSMV logically analyzes every possible path of the system, so that all possible timing variation cases of the cell cycle control circuit are checked. NuSMV concludes that a system design is hazard free if it would perform correctly for every possible set of inputs and parameter values. The program does not simulate all possibilities, but it achieves the equivalent result by exploring the finite, branching graph of all possibilities. This is a computationally efficient process. Checking the *C. crescentus* model with NuSMV requires less than 10 seconds of CPU time on a Lenovo X41 laptop computer.

Implementation in NuSMV

In the *C. crescentus* model in NuSMV, the state variables and update rules for the modular cell cycle functions are organized as a set of individual finite state machines. Some transitions have to wait until specific external conditions (e.g., a regulatory protein reaches a threshold, or a state machine reaches a certain state) are met before other transitions can be executed. There are state machines to model the steps of chromosome replication, the methylation states of certain promoters, stages of cell division, regulatory protein levels, and the phosphorylation state of various proteins.

The NuSMV input files used for the robustness checking of the *C. crescentus* cell cycle control circuit are available online at http://www.stanford.edu/group/caulobacter/CellModel. Additional information on the NuSMV implementation is provided in the embedded comments in the NuSMV input files. The README file explains how to run the input file, Caulobacter.txt, using NuSMV.

The example below is a simplified version of the chromosome replication state machine in the *C. crescentus* model that illustrates the modeling concepts.

The VAR declaration below defines a state variable that can have one of a list of possible values (which appear in the order that the states progress), according to the "init" and "next" functions specified later. In NuSMV, text after "--" are comments.

VAR
chromosome_replication_state : {
    pre_replication,   **-- single chromosome before replication starts**
    chromosome_rep_init,   **-- initiation of chromosome replication**
    dnaA,   **-- the replication fork replicates the dnaA gene,**
                         -- many states in between. See the full model for
                         -- omitted intermediate states.
    chromosome_rep_end   **-- the completion of chromosome replication**
                         -- and decatenation of the replicated
                         -- chromosomes
};

The ASSIGN declaration defines the actual replication state machine by specifying the initial state values (in the init declaration), and how the state variable is updated on each step (in the next declaration). The next declaration is used to determine the state values for the next step. The state machines in the *C. crescentus* model adhere to a particular convention: immediate transitions for instant reactions are written first, and then there are slow transitions with delays, which will not be evaluated until schedule determines the delay is over.

ASSIGN
-- The *C. crescentus* cell starts in the "pre_replication" state, where
-- there is a single chromosome before cell cycle division starts.
init(chromosome_replication_state) := pre_replication;

next(chromosome_replication_state) := case
   -- The next transition is immediate, since, after the
   -- decatenation of the two replicated chromosomes, the inner
   -- membrane compartmentalization instantly separates them in
   -- two compartments.
   chromosome_replication_state = chromosome_rep_end
       & (cytokinesis_state = Compartmentalization) : pre_replication;

-- The schedule determines if the delay is over.
-- Every transition below this must wait for the delay.
   !(schedule = chromosome_replication_delay) : chromosome_replication_state;

   -- chromosome replication is initiated when CtrA_P is low, DnaA
   -- is high, DnaB is high.
   chromosome_replication_state = pre_replication & !CtrA_P & DnaA

& DnaB
            : chromosome_rep_init;
         -- The dnaA gene is close to the ori.
         chromosome_replication_state = chromosome_rep_init : dnaA;
         -- The replication fork finishes replicating the rest of
         -- of the chromosome.
         chromosome_replication_state = dnaA : chromosome_rep_end
         -- If none of the above conditions is met, stay in the current state.
         1 : chromosome_replication_state;
esac;

NuSMV allows nondeterministic assignment, which means that a set of possible alternative values can be specified for a variable. Nondeterministic assignment allows the schedule variable to take on any of the state machines at each step; this enables the model to consider all possible delays.

The protein regulatory network is also modeled as a collection of small state machines, called "regulators," which correspond to logic gates in computer design. Below is generic NuSMV model for a regulator, which is instantiated for various proteins. When `promoter_activity` is 1, the promoter of the regulatory gene is activated. After an arbitrary `delay`, the accumulated protein `level` becomes 1 (high).

MODULE Regulator(promoter_activity, init_level, delay)
VAR level : boolean;
ASSIGN
  init(level) := init_level;
  next(level) :=
  case
    !delay : level;
    1 : promoter_activity;
  esac;

The generic gate model is instantiated for GcrA, whose promoter is active when `ctrA_P` is 0 and `DnaA` is 1.

gcrA : Regulator(!CtrA_P & DnaA, 0, (schedule = gcrA_delay));

This is a discrete abstraction of *gcrA* regulation. In a continuous ODE model it would be:

$$\frac{d([GcrA])}{dt} = \frac{\beta/V}{\{1+(\frac{[C_{d1}]}{[DnaA]+\varepsilon})^n\}\{1+(\frac{[CtrA \sim P]}{[C_{d2}]})^n\}} - [GcrA]\frac{\ln 2}{hl}$$

Where n, $[C_d]$ and β are Hill function parameters, V is the cell volume, and *hl* is the half-life of GcrA.
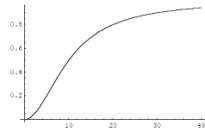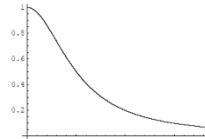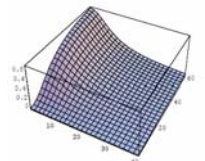
In the NuSMV model for the *C. crescentus* cell cycle control circuit, a dialect of temporal logic called CTL (for "Computation Tree Logic") is used to check whether the cell cycle is completed successfully. For example, the CTL statement " SPEC AG AF (cytokinesis_state = Divide & (AF cytokinesis_state != Divide)); " states that the cell divides repeatedly under all modeled conditions in perpetuity. More complicated checks were added to check if paths pass the critical cell cycle stages in the right succession order.

Tables

Table S1. Experiments done with *Caulobacter* cells and conclusions used to construct the model

Protein	Refs.	Conclusion used to construct the model
DnaA	(35)	DnaA is necessary for the initiation of DNA replication
DnaA	(3, 5)	DnaA activates *gcrA* transcription
DnaA	(3)	DnaA activates *ftsZ* transcription
DnaA	(3)	DnaA activates *dnaB* transcription
DnaA	(31)	DnaA is subject to cell cycle-regulated proteolysis
DnaA	(7)	*dnaA* transcription is activated when the *dnaA* promoter is fully-methylated
FtsZ	(36)	FtsZ is necessary for cell constriction
FtsZ	(37)	FtsZ is subject to cell cycle-regulated proteolysis
FtsA	(38)	FtsA is necessary for cell constriction
FtsA	(14)	FtsA is probably subject to cell cycle-regulated proteolysis
FtsQ	(14)	FtsQ is subject to cell cycle-regulated proteolysis
CcrM	(32)	CcrM is necessary for the methylation of the chromosome
CcrM	(39)	CcrM is subject to cell cycle-regulated proteolysis
CcrM	(9)	*ccrM* transcription is probably repressed when the *ccrM* promoter is fully-methylated
CtrA	(30)	CtrA is necessary to block the initiation of DNA replication
CtrA	(37)	CtrA represses *ftsZ* transcription
CtrA	(15)	CtrA activates *ftsQA* transcription
CtrA	(2, 5)	CtrA represses *gcrA* transcription
CtrA	(40)	CtrA represses *ctrA* transcription from the *ctrA*P1 promoter
CtrA	(40)	CtrA activates *ctrA* transcription from the *ctrA*P2 promoter
CtrA	(41)	CtrA activates *ccrM* transcription
CtrA	(27)	CtrA is subject to cell cycle-regulated proteolysis
CtrA	(10)	*ctrA* transcription is repressed when the *ctrA*P1 promoter is fully-methylated
CtrA	(27, 42)	CtrA needs to be phosphorylated to be active
GcrA	(2)	GcrA activates *dnaB* transcription
GcrA	(2)	GcrA activates *ctrA* transcription from *ctrA*P1
GcrA	(2)	GcrA represses *dnaA* expression
GcrA	(5)	GcrA is subject to cell cycle-regulated proteolysis
CckA	(24)	The CckA signal activates the phosphorylation of CtrA
CckA	(19)	The CckA signal represses the proteolysis of CtrA
CtrA	(15)	CtrA is not synthesized in predivisional cells if replication is inhibited

Table S2. Models used in the Simulink subsystem for protein production and activation levels

	Activator: $\dfrac{d[C]}{dt} = \dfrac{\beta/V}{1+(\dfrac{[C_d]}{[C_t]})^n}$
	Repressor: $\dfrac{d[C]}{dt} = \dfrac{\beta/V}{1+(\dfrac{[C_t]}{[C_d]})^n}$
	Activator-repressor: $\dfrac{d[C]}{dt} = \dfrac{\beta/V}{\{1+(\dfrac{[C_{d1}]}{[C_{t1}]})^{n1}\}\,\{1+(\dfrac{[C_{t2}]}{[C_{d2}]})^{n2}\}}$ Where n is the Hill coefficient, $[C_d]$ is the concentration of the transcriptional factor that yields half-maximal expression, $[C_t]$ is the concentration of the transcriptional factor, β is the maximal protein production rate , V is the volume of a *C. crescentus* cell. β/V for a specific gene remains approximately constant throughout the cell cycle because the effect of cell growth on concentrations is compensated by the increase of gene copy numbers. In the simulation model, n is a unit-less number, $[C_d]$ and $[C_t]$ are expressed in nM (nanomolar), β/V is expressed in nM/s (nanomolar per second).
	Degradation: $\dfrac{d[C]}{dt} = -\lambda \cdot [C] = -\dfrac{\ln 2}{hl}[C]$ Where hl is the half-life of the protein in min, and λ is the degradation rate constant in min^{-1}.

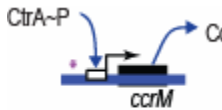| Specific forms for individual genes.	
	$$\frac{d([CtrA]+[CtrA \sim P])}{dt} = \frac{\beta_1/V}{\{1+(\frac{[C_{d1}]}{[GcrA]+\varepsilon})^n\}\{1+(\frac{[CtrA \sim P]}{[C_{d2}]})^n\}} \cdot [(1-\eta) \cdot m_{ctrA} + \eta]$$ $$+ \frac{\beta_2/V}{1+(\frac{[C_{d3}]}{[CtrA \sim P]+\varepsilon})^n} - [CtrA](\lambda_1 \cdot clpXP + \lambda_2)$$ $$\frac{d[CtrA \sim P]}{dt} = (k_f \cdot [CtrA] - k_r[CtrA \sim P])$$ We estimate from (10) that expression for the *ctrA P1* promoter is repressed by about 7-fold when the promoter is fully-methylated compared to when it is hemi-methylated. η is the relative expression level of a fully-methylated (OFF) *ctrA* P_1 promoter compared to that of a hemi-methylated (ON) *ctrA* P_1 promoter. m_{ctrA} is the methylation state of the *ctrA* P_1 promoter. $m_{ctrA}=0$ when it is fully-methylated and the maximal *ctrA* P_1 expression level is $\eta\beta_1$. $m_{ctrA}=1$ when it is hemi-methylated and the maximal *ctrA* P_1 expression level is β_1. β_2 is the maximal expression level of the *ctrA* P_2. *clpXP*=1 when the *clpXP* proteolysis machinery is active and *clpXP*=0 when it is inactive. The *m* and *clpXP* binary switches are set by inputs from Stateflow. The infinitesimal value ε is added to avoid divide-by-zero errors in the numerical integration routines. Since we assume that the speed of phosphorylation is far greater than the speed of protein synthesis when the phosphosignal is on, we use a linear equation to approximate the Michaelis-Menten rate equation for phosphorylation: $$\frac{d[CtrA \sim P]}{dt} = k_1 \cdot cckA \cdot [CtrA] + k_2 \cdot [CtrA] - k_3[CtrA \sim P]$$ k_1 is the phosphorylation rate of CtrA with the CckA phosphosignal present. The *cckA* binary switch from Stateflow is set to 1 when the CckA phosphosignal is active, and 0 when the CckA phosphosignal is inactive. k_2 is the phosphorylation rate of CtrA without the CckA phosphosignal (presumably very low). k_3 is the de-phosphorylation rate of CtrA~P.

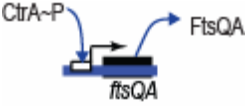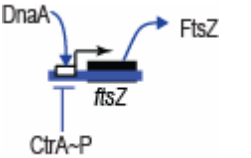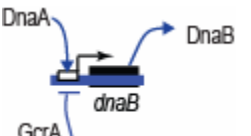|	
	$$\frac{d([GcrA])}{dt} = \frac{\beta/V}{\{1+(\frac{[C_{d1}]}{[DnaA]+\varepsilon})^n\}\{1+(\frac{[CtrA\sim P]}{[C_{d2}]})^n\}} -$$ $$[GcrA](\lambda_{sw} \cdot isSW + \lambda_2)$$ λ_{sw} is decided by the half-life of GcrA in swarmer cells, which is shorter than the half-life of GcrA in the stalked and pre-division cell stages. During the simulation, while the cell is in the swarmer stage, the binary variable *isSW* from Stateflow is set to 1.
	$$\frac{d([DnaA])}{dt} = \frac{\beta/V[(1-m_{dnaA}+\kappa \cdot m_{dnaA}]}{\{1+\frac{[DnaA]}{[C_{d1}]}\}\{1+(\frac{[GcrA]}{[C_{d2}]})^n\}} -$$ $$[DnaA](\lambda_{sw} \cdot isSW + \lambda_{st} \cdot isST + \lambda_2)$$ Expression of *dnaA* is repressed by about 3-fold when the *dnaA* promoter is hemi-methylated (7) compared to fully-methylated. In the simulation model, κ is the relative expression of a hemi-methylated (OFF) *dnaA* promoter compared to that of a fully-methylated (ON) *dnaA* promoter. m_{dnaA} is the methylation state of the *dnaA* promoter. When m_{dnaA} is 0, signifying that *dnaA* is fully-methylated, the maximal expression level is β. If m_{dnaA} is 1, or *dnaA* is hemi-methylated, the maximal expression *level is $\kappa\beta$.* Given the that there is one putative DnaA binding site in the sequence upstream of the *dnaA* coding sequence, it has been hypothesized that *dnaA* transcription is auto-regulated by DnaA (43), although this hypothesis does not affect the simulation outcome in any significant way. DnaA synthesis is also repressed by GcrA (2), probably by a post-transcriptional mechanism. We have approximated this effect with a Hill function. DnaA proteolysis is also cell cycle regulated (35). The proteolysis rate is set by the cell cycle stage parameters, *isSW* and *isST*.
	$$\frac{d([CcrM])}{dt} = \frac{\beta/V}{\{1+(\frac{[C_d]}{[CtrA\sim P]+\varepsilon})^n\}} \cdot m_{ccrM} - [CcrM](\lambda_{sw} \cdot isSW + \lambda_2)$$

CtrA~P → FtsQA *ftsQA*	$$\frac{d([FtsQA])}{dt} = \frac{\beta/V}{\{1+(\frac{[C_d]}{[CtrA \sim P]+\varepsilon})^n\}} - [FtsQA](\lambda_{sw} \cdot isSW + \lambda_2)$$ There is a second *ftsA* only promoter which is relatively weak and ignored by the model (44).
DnaA → FtsZ *ftsZ* CtrA~P	$$\frac{d([FtsZ])}{dt} = \frac{\beta/V}{\{1+(\frac{[C_{d1}]}{[DnaA]+\varepsilon})^n\}\{1+(\frac{[CtrA \sim P]}{[C_{d2}]})^n\}} -$$ $$[FtsZ](\lambda_{pd} \cdot isPD + \lambda_2)$$ The *ftsZ* promoter is activated by DnaA (3) and repressed by CtrA~P (37). FtsZ has a shorter half-life in the pre-divisional stage which is modeled by an added degradation term activated only in the predivisional cell stage, when *isPD* is set to 1 by the Stateflow cell stage monitor.
DnaA → DnaB *dnaB* GcrA	$$\frac{d([DnaB])}{dt} = \frac{\beta/V}{\{1+(\frac{[C_{d1}]}{[DnaA]+\varepsilon})^n\}\{1+(\frac{[GcrA]}{[C_{d2}]})^n\}} - [DnaB]\lambda$$ The *dnaB* promoter is activated by DnaA (3) and repressed by GcrA (2).

Table S3: Parameter values

Table S3A. Model parameters with experimentally measured values

Symbol	Parameter	Value	Units	Source or rationale
cCcrM0	Concentration of CcrM in swarmer cells	0	nM	(45)
cCtrA0	Concentration of CtrA in swarmer cells	20900	nM	9500 CtrA molecules are present in the swarmer cell (42) or about 20900 nM.
cFtsA0	Concentration of FtsA in swarmer cells	0	nM	(14)
cFtsZ0	Concentration of FtsZ in swarmer cells	0	nM	(37)
cGcrA0	Concentration of GcrA in swarmer cells	0	nM	(2)
cMethylCcrM	Concentration of CcrM during chromosome methylation	6600	nM	3000 molecules in the late PD cell (46) or about 6600 nM.
hlCcrMc	CcrM half-life	15	min	(39)
hlCtrAc	CtrA half-life	52	min	Measured in mixed population (18).
hlCtrAf	CtrA half-life during proteolysis by ClpXP	3	min	CtrA half-life is less than 5 minutes in the stalked cell (27)
hlDnaA_sw	DnaA half-life in the swarmer cell	45	min	(31)
hlDnaAc	DnaA half-life in the stalked cell	100	min	(31)
hlDnaAc_starve	DnaA half-life during starvation	10	min	The half-life of DnaA is 10 minutes during carbon starvation and 15 minutes during nitrogen starvation (31).
hlFtsAc_st	FtsA half-life in the stalked cell	55	min	(14)
hlFtsAc_sw	FtsA half-life in the swarmer cell	13	min	(14)
hlFtsZc	FtsZ half-life in the swarmer cell and the stalked cell	80	min	(37)
hlFtsZc_pd	FtsZ half-life in the pre-divisional	20	min	(37)
hlGcrAc_st	GcrA half-life in the stalked cell	42	min	(5)
hlGcrAc_sw	GcrA half-life in the	10.5	min	(5)

	swarmer cell			
pctrAP1MethRatio	The ratio of transcription rates between the fully-methylated and the hemi-methylated *ctrA* P1 promoter.	0.15		(10)
pdnaAMethRatio	The ratio between the hemi-methylated transcription rate and the fully-methylated transcription rate from the *dnaA* promoter.	0.3		(7) This ratio is used in the model to approximate the transcription rate of the hemi-methylated *dnaA* promoter.
tcckA_reloc	Time between the initiation of chromosome replication and CckA re-localization	60	min	(19) CckA is relocalized approximately 80 minutes into the cell cycle. The swarmer stage takes 20 so CckA relocalizes 60 minutes into chromosome replication.
tchro	Time required for chromosome replication	80	min	(28) Scaled for a 135 minute cell cycle.
tftzRing	Time required for cytokinesis	30	min	(47)
tftzRingPinOff	Time between the start of constriction and compartmentalization	12	min	(17, 47)
tMethylWindow	Average time for the DNA to be methylated once CcrM concentration reaches cMethylCcrM	10	min	Since there is a 20 minute window (46) when DNA is being methylated by a high concentration of active CcrM molecules, we chose 10 minutes as the average time it takes for the chromosome to be methylated.
tsw2st	Duration of the swarmer stage	20	min	(28) Scaled for a 135 minute cell cycle.
zpctrA	The relative location of the *ctrA* gene on the chromosome	0.3		0 is the *ori*, and 1 is the *terminus* of the chromosome (48)
zpccrM	The relative location of the *ccrM* gene on the chromosome	0.25		0 is the *ori*, and 1 is the *terminus* of the chromosome (48)
zpdnaA	The relative location of the *dnaA* gene on the chromosome	0.1		0 is the *ori*, and 1 is the *terminus* of the chromosome (48).

Table S3B. Model parameters with estimated values

Symbol	Parameter	Value	Units	Source or rationale
cChroCtrA	CtrA threshold level for initiating DNA replication	110	nM	There are 5 CtrA binding sites in the *Cori.* CtrA blocks DNA replication by binding to these sites (30). 50 CtrA molecules per cell is assumed to be adequate to ensure blocking, which translates into 110 nM.
cChroDnaA	DnaA threshold level for initiating DNA replication	440	nM	DnaA is necessary for replisome assembly (35). The simulation is not sensitive to this value as long as it is a small fraction of the maximum DnaA level.440 nM corresponds to 200 molecules per cell.
cChroDnaB	DnaB threshold for initiating DNA replication	440	nM	This concentration is equivalent to 200 molecules per cell.
cCtrAP0	Initial concentration of CtrA~P	10450	nM	This concentration is consistent with the observation that phosphorylation of CtrA is less active in the swarmer stage (49)
cCytoFtsQA	FtsQA threshold for initiating cytokinesis	660	nM	This concentration is equivalent to 300 molecules per cell.
cDnaA0	Initial concentration of DnaA	2200	nM	This concentration is equivalent to 1000 molecules per cell.
cDnaB0	Initial concentration of DnaB	2200	nM	This concentration is equivalent to 1000 molecules per cell.
cHalfCtrA	Concentration of CtrA~P that yields half-maximal expression of CtrA-regulated genes.	1760	nM	This concentration is equivalent to 800 molecules per cell.
cHalfDef	Default level of transcriptional factors that yields half-maximal expression of target genes	660	nM	This concentration is equivalent to 300 molecules per cell.
cZringFtsZ	Minimum level of FtsZ required for forming the FtsZ ring	660	nM	This concentration is equivalent to 300 molecules per cell.
hcDef	Default Hill function coefficient	2		This default value is assumed for all protein synthesis in the model, including CtrA. For future model development, promoter-specific hill coefficient can be specified as hcX for protein X.
hlCcrMc_sw	CcrM half-life in the swarmer cell	3	min	The half-life of CcrM in Table 2A was measured in a mixed population. Western blot of CcrM shows that CcrM is fully depleted in the swarmer cell in a relatively short time, so the half-life of CcrM is estimated to be 3

				minutes in the swarmer cell.
hlDnaAc_degrade	DnaA half-life during chromosome replication initiation	15	min	The levels of DnaA decrease during the early stage of chromosome replication, as seen on Western blots of DnaA as a function of the cell cycle.
hlDnaBc	DnaB half-life	10	min	DnaB in this model represents a collection of proteins that are responsible for initiating chromosome replication.
hlPhos_f_e	Time for half of the CtrA molecules to be phosphorylated when the cckA signal is ON.	0.1	min	The value is chosen because phosphorylation reactions are much faster than transcription and degradation reactions.
hlPhos_f_ne	Time for half of the CtrA molecules to be phosphorylated when the cckA signal is OFF.	150	min	CtrA is not actively phosphorylated without the active kinase CckA. (24)
hlPhos_r_np	Time for half of the CtrA~P molecules to become dephosphorylated without phosphatase present	3	min	We assume that CtrA gradually becomes inactive when the *cckA* signal is OFF.
p1ctrA	Maximum synthesis rate of CtrA from the *ctrA* P1 promoter	6.6	nM/s	The maximum expression level of p2ctrA is roughly 3 times that of p1ctrA (10).
P2ctrA	Maximum synthesis rate of CtrA from the *ctrA* P2 promoter	19.8	nM/s	The maximum expression level of p2ctrA is roughly 3 times that of p1ctrA (10).
pccrM	Maximum synthesis rate of CcrM from the *ccrM* promoter	13.2	nM/s	Estimated from western blots and (46)
pdnaA	Maximum synthesis rate of DnaA from the *dnaA* promoter	1.76	nM/s	The absolute value does not affect simulation outcome after normalization.
pdnaB	Maximum synthesis rate of DnaB from the *dnaB* promoter	1.1	nM/s	The absolute value does not affect simulation outcome after normalization.
pftsA	Maximum synthesis rate of FtsA from the *ftsQA* promoter	1.1	nM/s	The absolute value does not affect simulation outcome after normalization.
pftsZ	Maximum synthesis rate of FtsZ from the *ftsZ* promoter	1.1	nM/s	The absolute value does not affect simulation outcome after normalization.
pgcrA	Maximum synthesis rate of GcrA from the *gcrA* promoter	2.2	nM/s	The absolute value does not affect simulation outcome after normalization.

Table S3C. Parameters for mutant simulations and simulation controls

Symbol	Parameter	Value	Units	Source or rationale
isAlwaysCtrAP	If set to 1, CtrA is always in its active form.	0		It is for mutant simulations that mimic an always active CtrA.
pccrMoe	Synthesis rate of the constitutive promoter driving *ccrM* expression in mutant simulation	0	nM/s	Set to a non-zero number such as 100 for mutant simulation.
pctrAoe	Synthesis rate of the constitutive promoter driving *ctrA* expression in mutant simulation	0	nM/s	Set to a non-zero number such as 100 for mutant simulation.
pdnaAoe	Synthesis rate of the constitutive promoter driving *dnaA* expression in mutant simulation	0	nM/s	Set to a non-zero number such as 100 for mutant simulation.
pgcrAoe	Synthesis rate of the constitutive promoter driving *gcrA* expression in mutant simulation	0	nM/s	Set to a non-zero number such as 100 for mutant simulation.
pxylose	For mutant simulation, if pxylose is 1, the constitutive promoter is enabled at the time specified by txylose.	0		Provides an extra switch to activate or deactivate the constitutive promoter during a mutant simulation.
t_trackST	At time t_trackST, the simulation switches the type of the cell it tracks according to t_trackST	1		Simulation program parameter
trackST	A binary switch that sets the simulation to track the stalked cell (=1) or the swarmer cell (=0)	0		Simulation program parameter
txylose	Time to induce the constitutive promoter in mutant simulation.	1	min	The value determines the time point when a constitutive promoter is induced in mutant simulations.

Table S4: mutant phenotypes

Characteristics of mutant strains	*Genotypes of mutant strains*	Refs	Phenotypes *in vivo*	Parameters changed from wild-type parameters for mutant simulations
Strain where GcrA can be depleted (LS3707)	CB15N ΔgcrA Pxyl::gcrA	(2)	The cell cycle is arrested at the stalked cell stage, and cells finally die in the absence of GcrA.	Maximum GcrA synthesis rate from the *gcrA* promoter pgcrA=0nM/s
Strain that accumulates CcrM constitutively (LS1)	CB15N PlacZ::ccrM	(32)	Cells are slightly elongated and accumulate supplementary copies of the chromosome.	CcrM synthesis rate from a constitutive promoter added in the model pccrMoe=100nM/s
Strain that can accumulate stable and constitutively active mutant CtrA proteins	CB15N pXylX:: ctrAD51EΔ3Ω	(27)	Cells do not initiate DNA replication and do not divide. Cells elongate before dying.	Binary switch controlling the phosphorylation state of CtrA and the protein half-life of CtrA under active proteolysis by ClpX isAlwaysCtrAP=1 hlCtrAf=200 min
Strain where the *ctrA* gene is moved to a position next to the terminus of replication of the chromosome (LS3355)	CB15N ctrAΔ2::pAR358	(10)	Cell size is sometimes irregular	Relative location of the *ctrA* gene on the chromosome zpctrA=1

References

1.   Laub, M. T., Chen, S. L., Shapiro, L., & McAdams, H. H. (2002) Genes directly controlled by CtrA, a master regulator of the *Caulobacter* cell cycle *Proc Natl Acad Sci U S A* **99,** 4632-4637.

2.   Holtzendorff, J., Hung, D., Brende, P., Reisenauer, A., Viollier, P. H., McAdams, H. H., & Shapiro, L. (2004) Oscillating global regulators control the genetic circuit driving a bacterial cell cycle *Science* **304,** 983-987.

3.   Hottes, A. K., Shapiro, L., & McAdams, H. H. (2005) DnaA coordinates replication initiation and cell cycle transcription in *Caulobacter crescentus Mol Microbiol* **58,** 1340-1353.

4.   Collier, J. & Shapiro, L. (2007) Spatial complexity and control of a bacterial cell cycle *Curr Opin Biotechnol* **18,** 333-340.

5.   Collier, J., Murray, S. R., & Shapiro, L. (2006) DnaA couples DNA replication and the expression of two cell cycle master regulators *Embo J* **25,** 346-356.

6.   Reisenauer, A., Kahng, L. S., McCollum, S., & Shapiro, L. (1999) Bacterial DNA methylation: a cell cycle regulator? *J Bacteriol* **181,** 5135-5139.

7.   Collier, J., McAdams, H. H., & Shapiro, L. (2007) A DNA methylation ratched governs progression through a bacterial cell cycle *Proceedings of the National Academy, USA***,** In press.

8.   Degnen, S. T. & Newton, A. (1972) Dependence of cell division on the completion of chromosome replication in *Caulobacter J Bacteriol* **110,** 852-856.

9.   Stephens, C. M., Zweiger, G., & Shapiro, L. (1995) Coordinate cell cycle control of a Caulobacter DNA methyltransferase and the flagellar genetic hierarchy *J Bacteriol* **177,** 1662-1669.

10.   Reisenauer, A. & Shapiro, L. (2002) DNA methylation affects the cell cycle transcription of the CtrA global regulator in *Caulobacter Embo J* **21,** 4969-4977.

11.   Wright, R., Stephens, C., & Shapiro, L. (1997) The CcrM DNA methyltransferase is widespread in the alpha subdivision of proteobacteria, and its essential functions are conserved in *Rhizobium meliloti* and *Caulobacter crescentus J Bacteriol* **179,** 5869-5877.

12.   Shier, V. K., Hancey, C. J., & Benkovic, S. J. (2001) Identification of the active oligomeric state of an essential adenine DNA methyltransferase from *Caulobacter crescentus J Biol Chem* **276,** 14744-14751.

13.   Margolin, W. (2005) FtsZ and the division of prokaryotic cells and organelles *Nat Rev Mol Cell Biol* **6,** 862-871.

14.   Martin, M. E., Trimble, M. J., & Brun, Y. V. (2004) Cell cycle-dependent abundance, stability and localization of FtsA and FtsQ in *Caulobacter crescentus Mol Microbiol* **54,** 60-74.

15.   Wortinger, M., Sackett, M. J., & Brun, Y. V. (2000) CtrA mediates a DNA replication checkpoint that prevents cell division in *Caulobacter crescentus Embo J* **19,** 4503-4512.

16.   Judd, E. M., Comolli, L. R., Chen, J. C., Downing, K. H., Moerner, W. E., & McAdams, H. H. (2005) Distinct constrictive processes, separated in time and space, divide *Caulobacter* inner and outer membranes *J Bacteriol* **187,** 6874-6882.

17. Judd, E. M., Ryan, K. R., Moerner, W. E., Shapiro, L., & McAdams, H. H. (2003) Fluorescence bleaching reveals asymmetric compartment formation prior to cell division in *Caulobacter Proc Natl Acad Sci U S A* **100,** 8235-8240.
18. McGrath, P. T., Iniesta, A. A., Ryan, K. R., Shapiro, L., & McAdams, H. H. (2006) A dynamically localized protease complex and a polar specificity factor control a cell cycle master regulator *Cell* **124,** 535-547.
19. Iniesta, A. A., McGrath, P. T., Reisenauer, A., McAdams, H. H., & Shapiro, L. (2006) A phospho-signaling pathway controls the localization and activity of a protease complex critical for bacterial cell cycle progression *Proc Natl Acad Sci U S A*.
20. Biondi, E. G., Reisinger, S. J., Skerker, J. M., Arif, M., Perchuk, B. S., Ryan, K. R., & Laub, M. T. (2006) Regulation of the bacterial cell cycle by an integrated genetic circuit *Nature* **444,** 899-904.
21. McAdams, H. H. & Shapiro, L. (2003) A bacterial cell-cycle regulatory network operating in time and space *Science* **301,** 1874-1877.
22. McGrath, P. T., Viollier, P., & McAdams, H. H. (2004) Setting the pace: mechanisms tying *Caulobacter* cell-cycle progression to macroscopic cellular events *Curr Opin Microbiol* **7,** 192-197.
23. Matroule, J. Y., Lam, H., Burnette, D. T., & Jacobs-Wagner, C. (2004) Cytokinesis monitoring during development; rapid pole-to-pole shuttling of a signaling protein by localized kinase and phosphatase in *Caulobacter Cell* **118,** 579-590.
24. Jacobs, C., Domian, I. J., Maddock, J. R., & Shapiro, L. (1999) Cell cycle-dependent polar localization of an essential bacterial histidine kinase that controls DNA replication and cell division *Cell* **97,** 111-120.
25. Mathworks, Simulink-Simulation and model-based design. http://www.mathworks.com/products/simulink/
26. Mathworks, Stateflow 6.5-Design and simulate statemachines and control logic. http://www.mathworks.com/products/stateflow/
27. Domian, I. J., Quon, K. C., & Shapiro, L. (1997) Cell type-specific phosphorylation and proteolysis of a transcriptional regulator controls the G1-to-S transition in a bacterial cell cycle *Cell* **90,** 415-424.
28. Keiler, K. C. & Shapiro, L. (2003) TmRNA is required for correct timing of DNA replication in *Caulobacter crescentus J Bacteriol* **185,** 573-580.
29. Siam, R., Brassinga, A. K., & Marczynski, G. T. (2003) A dual binding site for integration host factor and the response regulator CtrA inside the *Caulobacter crescentus* replication origin *J Bacteriol* **185,** 5563-5572.
30. Quon, K. C., Yang, B., Domian, I. J., Shapiro, L., & Marczynski, G. T. (1998) Negative control of bacterial DNA replication by a cell cycle regulatory protein that binds at the chromosome origin *Proc Natl Acad Sci U S A* **95,** 120-125.
31. Gorbatyuk, B. & Marczynski, G. T. (2005) Regulated degradation of chromosome replication proteins DnaA and CtrA in *Caulobacter crescentus Mol Microbiol* **55,** 1233-1245.
32. Zweiger, G., Marczynski, G., & Shapiro, L. (1994) A *Caulobacter* DNA methyltransferase that functions only in the predivisional cell *J Mol Biol* **235,** 472-485.
33. Clarke, E. M., Emerson, E. A., & Sistla, A. P. (1986) Automatic verification of finite-state concurrent systems using temporal logic specifications *ACM Transactions on Programming Languages and Systems* **8,** 244 - 263

34. Cimatti, A., Clarke, E. M., Giunchiglia, E., Giunchiglia, F., Pistore, M., Roveri, M., Sebastiani, R., & Tacchella, A. (2002) in *International Conference on Computer-Aided Verification (CAV 2002)* (Copenhagen, Denmark).

35. Gorbatyuk, B. & Marczynski, G. T. (2001) Physiological consequences of blocked *Caulobacter crescentus* dnaA expression, an essential DNA replication gene *Mol Microbiol* **40,** 485-497.

36. Wang, Y., Jones, B. D., & Brun, Y. V. (2001) A set of ftsZ mutants blocked at different stages of cell division in Caulobacter *Mol Microbiol* **40,** 347-360.

37. Kelly, A. J., Sackett, M. J., Din, N., Quardokus, E., & Brun, Y. V. (1998) Cell cycle-dependent transcriptional and proteolytic regulation of FtsZ in *Caulobacter Genes Dev* **12,** 880-893.

38. Osley, M. A. & Newton, A. (1977) Mutational analysis of developmental control in Caulobacter crescentus *Proc Natl Acad Sci U S A* **74,** 124-128.

39. Wright, R., Stephens, C., Zweiger, G., Shapiro, L., & Alley, M. R. (1996) *Caulobacter* Lon protease has a critical role in cell-cycle control of DNA methylation *Genes Dev* **10,** 1532-1542.

40. Domian, I. J., Reisenauer, A., & Shapiro, L. (1999) Feedback control of a master bacterial cell-cycle regulator *Proc Natl Acad Sci U S A* **96,** 6648-6653.

41. Reisenauer, A., Quon, K., & Shapiro, L. (1999) The CtrA response regulator mediates temporal control of gene expression during the *Caulobacter* cell cycle *J Bacteriol* **181,** 2430-2439.

42. Quon, K. C., Marczynski, G. T., & Shapiro, L. (1996) Cell cycle control by an essential bacterial two-component signal transduction protein *Cell* **84,** 83-93.

43. Zweiger, G. & Shapiro, L. (1994) Expression of Caulobacter dnaA as a function of the cell cycle *J Bacteriol* **176,** 401-408.

44. Sackett, M. J., Kelly, A. J., & Brun, Y. V. (1998) Ordered expression of *ftsQA* and *ftsZ* during the *Caulobacter crescentus* cell cycle *Mol Microbiol* **28,** 421-434.

45. Stephens, C., Reisenauer, A., Wright, R., & Shapiro, L. (1996) A cell cycle-regulated bacterial DNA methyltransferase is essential for viability *Proc Natl Acad Sci U S A* **93,** 1210-1214.

46. Berdis, A. J., Lee, I., Coward, J. K., Stephens, C., Wright, R., Shapiro, L., & Benkovic, S. J. (1998) A cell cycle-regulated adenine DNA methyltransferase from *Caulobacter crescentus* processively methylates GANTC sites on hemimethylated DNA *Proc Natl Acad Sci U S A* **95,** 2874-2879.

47. Thanbichler, M. & Shapiro, L. (2006) MipZ, a spatial regulator coordinating chromosome segregation with cell division in *Caulobacter Cell* **126,** 147-162.

48. Nierman, W. C., Feldblyum, T. V., Laub, M. T., Paulsen, I. T., Nelson, K. E., Eisen, J. A., Heidelberg, J. F., Alley, M. R., Ohta, N., Maddock, J. R.*, et al.* (2001) Complete genome sequence of Caulobacter crescentus *Proc Natl Acad Sci U S A* **98,** 4136-4141.

49. Jacobs, C., Ausmees, N., Cordwell, S. J., Shapiro, L., & Laub, M. T. (2003) Functions of the CckA histidine kinase in *Caulobacter* cell cycle control *Mol Microbiol* **47,** 1279-1290.